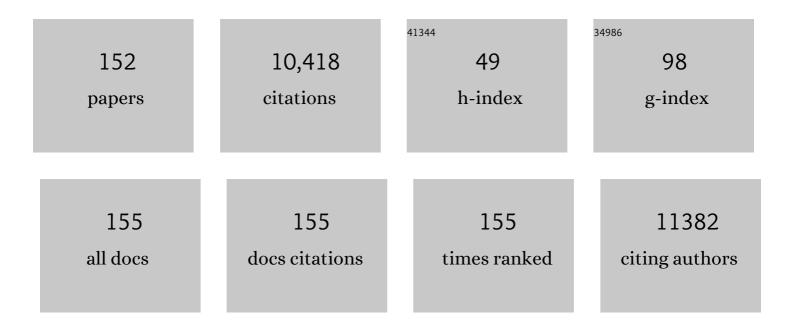
## Jia-Tao Zhang

List of Publications by Year in descending order

Source: https://exaly.com/author-pdf/1155870/publications.pdf Version: 2024-02-01



ΙΙΑ-ΤΛΟ ΖΗΛΝΟ

#	Article	IF	CITATIONS
1	Nearly Monodisperse Cu2O and CuO Nanospheres:Â Preparation and Applications for Sensitive Gas Sensors. Chemistry of Materials, 2006, 18, 867-871.	6.7	1,053
2	Engineering unsymmetrically coordinated Cu-S1N3 single atom sites with enhanced oxygen reduction activity. Nature Communications, 2020, 11, 3049.	12.8	537
3	Modulating the local coordination environment of single-atom catalysts for enhanced catalytic performance. Nano Research, 2020, 13, 1842-1855.	10.4	532
4	Nonepitaxial Growth of Hybrid Core-Shell Nanostructures with Large Lattice Mismatches. Science, 2010, 327, 1634-1638.	12.6	514
5	Bismuth Single Atoms Resulting from Transformation of Metal–Organic Frameworks and Their Use as Electrocatalysts for CO <sub>2</sub> Reduction. Journal of the American Chemical Society, 2019, 141, 16569-16573.	13.7	501
6	Surface Enhanced Raman Scattering Effects of Silver Colloids with Different Shapes. Journal of Physical Chemistry B, 2005, 109, 12544-12548.	2.6	359
7	Atomic interface effect of a single atom copper catalyst for enhanced oxygen reduction reactions. Energy and Environmental Science, 2019, 12, 3508-3514.	30.8	278
8	In Situ Phosphatizing of Triphenylphosphine Encapsulated within Metal–Organic Frameworks to Design Atomic Co <sub>1</sub> –P <sub>1</sub> N <sub>3</sub> Interfacial Structure for Promoting Catalytic Performance. Journal of the American Chemical Society, 2020, 142, 8431-8439.	13.7	259
9	Engineering Isolated Mn–N <sub>2</sub> C <sub>2</sub> Atomic Interface Sites for Efficient Bifunctional Oxygen Reduction and Evolution Reaction. Nano Letters, 2020, 20, 5443-5450.	9.1	249
10	Discovery of main group single Sb–N <sub>4</sub> active sites for CO <sub>2</sub> electroreduction to formate with high efficiency. Energy and Environmental Science, 2020, 13, 2856-2863.	30.8	245
11	Tailoring light–matter–spin interactions in colloidal hetero-nanostructures. Nature, 2010, 466, 91-95. Synthesis and Crystal Structures of the Ligandâ€Stabilized Silver Chalcogenide Clusters	27.8	242
12	[Ag <sub>154</sub> Se <sub>77</sub> (dppxy) <sub>18</sub> ], [Ag <sub>320</sub> (S <i>t</i> Bu) <sub>60</sub> S <sub>130</sub> (dppp) <sub>12</sub> ], [Ag <sub>352</sub> S <sub>128</sub> (S <i>t</i> C <sub>5</sub> H <sub>11</sub> ) <sub>96</sub> ], and [Ag <sub>490</sub> S <sub>188</sub> (S <i>t</i> C <sub>5</sub> H <sub>11</sub> ) <sub>114</sub> ].	13.8	241
13	Angewandte Chemie - International Edition, 2008, 47, 1326-1331. Design of a Singleâ€Atom Indium <sup>δ+</sup> –N <sub>4</sub> Interface for Efficient Electroreduction of CO <sub>2</sub> to Formate. Angewandte Chemie - International Edition, 2020, 59, 22465-22469.	13.8	232
14	Structurally Wellâ€Defined Au@Cu <sub>2â^'</sub> <i><sub>x</sub></i> S Core–Shell Nanocrystals for Improved Cancer Treatment Based on Enhanced Photothermal Efficiency. Advanced Materials, 2016, 28, 3094-3101.	21.0	228
15	Nanointerface Chemistry: Lattice-Mismatch-Directed Synthesis and Application of Hybrid Nanocrystals. Chemical Reviews, 2020, 120, 2123-2170.	47.7	206
16	Synthetic strategies of supported atomic clusters for heterogeneous catalysis. Nature Communications, 2020, 11, 5884.	12.8	174
17	Catalytic Nanomaterials toward Atomic Levels for Biomedical Applications: From Metal Clusters to Single-Atom Catalysts. ACS Nano, 2021, 15, 2005-2037.	14.6	148
18	Controlling Structural Symmetry of a Hybrid Nanostructure and its Effect on Efficient Photocatalytic Hydrogen Evolution. Advanced Materials, 2014, 26, 1387-1392.	21.0	142

#	Article	IF	CITATIONS
19	Engineering the Local Atomic Environments of Indium Singleâ€Atom Catalysts for Efficient Electrochemical Production of Hydrogen Peroxide. Angewandte Chemie - International Edition, 2022, 61, .	13.8	127
20	Visually resolving the direct Z-scheme heterojunction in CdS@ZnIn2S4 hollow cubes for photocatalytic evolution of H2 and H2O2 from pure water. Applied Catalysis B: Environmental, 2021, 293, 120213.	20.2	123
21	Metal@semiconductor core-shell nanocrystals with atomically organized interfaces for efficient hot electron-mediated photocatalysis. Nano Energy, 2018, 48, 44-52.	16.0	118
22	Stretchable supercapacitor at â^'30 °C. Energy and Environmental Science, 2021, 14, 3075-3085.	30.8	114
23	Hollow core photonic crystal fiber surface-enhanced Raman probe. Applied Physics Letters, 2006, 89, 204101.	3.3	113
24	Engineering a metal–organic framework derived Mn–N <sub>4</sub> –C <sub>x</sub> S <sub>y</sub> atomic interface for highly efficient oxygen reduction reaction. Chemical Science, 2020, 11, 5994-5999.	7.4	113
25	Nature-Inspired Na <sub>2</sub> Ti <sub>3</sub> O <sub>7</sub> Nanosheets-Formed Three-Dimensional Microflowers Architecture as a High-Performance Anode Material for Rechargeable Sodium-Ion Batteries. ACS Applied Materials & Interfaces, 2017, 9, 11669-11677.	8.0	103
26	Amorphous molybdenum sulfide nanocatalysts simultaneously realizing efficient upgrading of residue and synergistic synthesis of 2D MoS <sub>2</sub> nanosheets/carbon hierarchical structures. Green Chemistry, 2020, 22, 44-53.	9.0	102
27	Laser photonic-reduction stamping for graphene-based micro-supercapacitors ultrafast fabrication. Nature Communications, 2020, 11, 6185.	12.8	93
28	Formation of crystalline carbon nitride powder by a mild solvothermal method. Journal of Materials Chemistry, 2003, 13, 1241.	6.7	91
29	Two-Dimensional All-in-One Sulfide Monolayers Driving Photocatalytic Overall Water Splitting. Nano Letters, 2021, 21, 6228-6236.	9.1	88
30	Efficient Plasmonic Au/CdSe Nanodumbbell for Photoelectrochemical Hydrogen Generation beyond Visible Region. Advanced Energy Materials, 2019, 9, 1803889.	19.5	85
31	Cation/Anion Exchange Reactions toward the Syntheses of Upgraded Nanostructures: Principles and Applications. Matter, 2020, 2, 554-586.	10.0	81
32	Versatile Strategy for Precisely Tailored Core@Shell Nanostructures with Single Shell Layer Accuracy: The Case of Metallic Shell. Nano Letters, 2009, 9, 4061-4065.	9.1	76
33	Oxygen vacancy engineering of self-doped SnO <sub>2â^'x</sub> nanocrystals for ultrasensitive NO <sub>2</sub> detection. Journal of Materials Chemistry C, 2020, 8, 487-494.	5.5	76
34	Bambooâ€Like Nitrogenâ€Doped Carbon Nanotubes with Co Nanoparticles Encapsulated at the Tips: Uniform and Largeâ€Scale Synthesis and Highâ€Performance Electrocatalysts for Oxygen Reduction. Chemistry - A European Journal, 2015, 21, 14022-14029.	3.3	74
35	Rigid three-dimensional Ni <sub>3</sub> S <sub>4</sub> nanosheet frames: controlled synthesis and their enhanced electrochemical performance. RSC Advances, 2015, 5, 8422-8426.	3.6	70
36	Heterovalentâ€Dopingâ€Enabled Efficient Dopant Luminescence and Controllable Electronic Impurity Via a New Strategy of Preparing IIâ^'VI Nanocrystals. Advanced Materials, 2015, 27, 2753-2761.	21.0	67

#	Article	IF	CITATIONS
37	Excitonic pathway to photoinduced magnetism in colloidal nanocrystals with nonmagnetic dopants. Nature Nanotechnology, 2018, 13, 145-151.	31.5	64
38	Hydrothermal Cation Exchange Enabled Gradual Evolution of Au@ZnS–AgAuS Yolk–Shell Nanocrystals and Their Visible Light Photocatalytic Applications. Advanced Science, 2018, 5, 1700376.	11.2	64
39	Hydrophilic Doped Quantum Dots "Ink―and Their Inkjetâ€Printed Patterns for Dual Mode Anticounterfeiting by Reversible Cation Exchange Mechanism. Advanced Functional Materials, 2019, 29, 1808762.	14.9	63
40	Plasmon enhanced photoelectrochemical sensing of mercury (II) ions in human serum based on Au@Ag nanorods modified TiO2 nanosheets film. Biosensors and Bioelectronics, 2016, 79, 866-873.	10.1	60
41	Ultrathin single-crystalline TiO2 nanosheets anchored on graphene to be hybrid network for high-rate and long cycle-life sodium battery electrode application. Journal of Power Sources, 2017, 342, 405-413.	7.8	60
42	Heterovalent Doping in Colloidal Semiconductor Nanocrystals: Cation-Exchange-Enabled New Accesses to Tuning Dopant Luminescence and Electronic Impurities. Journal of Physical Chemistry Letters, 2017, 8, 4943-4953.	4.6	59
43	Hybrid Plasmonic Nanodumbbells Engineering for Multi-Intensified Second Near-Infrared Light Induced Photodynamic Therapy. ACS Nano, 2021, 15, 8694-8705.	14.6	59
44	Noble metal nanoclusters and their in situ calcination to nanocrystals: Precise control of their size and interface with TiO2 nanosheets and their versatile catalysis applications. Nano Research, 2016, 9, 1763-1774.	10.4	57
45	Hydrothermal One-Step Synthesis of Highly Dispersed M-Phase VO <sub>2</sub> Nanocrystals and Application to Flexible Thermochromic Film. ACS Applied Materials & Interfaces, 2018, 10, 28627-28634.	8.0	56
46	Controllable Synthesis of Nanosized Amorphous MoS <i><sub>x</sub></i> Using Temporally Shaped Femtosecond Laser for Highly Efficient Electrochemical Hydrogen Production. Advanced Functional Materials, 2019, 29, 1806229.	14.9	54
47	Controlled Synthesis of Co@N-Doped Carbon by Pyrolysis of ZIF with 2-Aminobenzimidazole Ligand for Enhancing Oxygen Reduction Reaction and the Application in Zn–Air Battery. ACS Applied Materials & Interfaces, 2020, 12, 11693-11701.	8.0	54
48	Highly Selective Photoreduction of CO <sub>2</sub> with Suppressing H <sub>2</sub> Evolution by Plasmonic Au/CdSe–Cu <sub>2</sub> O Hierarchical Nanostructures under Visible Light. Small, 2020, 16, e2000426.	10.0	53
49	A self-healing zinc ion battery under -20 °C. Energy Storage Materials, 2022, 44, 517-526.	18.0	53
50	Revealing the effect of interfacial electron transfer in heterostructured Co <sub>9</sub> S <sub>8</sub> @NiFe LDH for enhanced electrocatalytic oxygen evolution. Journal of Materials Chemistry A, 2021, 9, 12244-12254.	10.3	52
51	Phosphineâ€Initiated Cation Exchange for Precisely Tailoring Composition and Properties of Semiconductor Nanostructures: Old Concept, New Applications. Angewandte Chemie - International Edition, 2015, 54, 3683-3687.	13.8	51
52	A Flexible Aqueous Zinc–lodine Microbattery with Unprecedented Energy Density. Advanced Materials, 2022, 34, e2109450.	21.0	49
53	Surface micro/nanostructure evolution of Au–Ag alloy nanoplates: Synthesis, simulation, plasmonic photothermal and surface-enhanced Raman scattering applications. Nano Research, 2016, 9, 876-885.	10.4	43
54	Boron-doped microporous nano carbon as cathode material for high-performance Li-S batteries. Nano Research, 2017, 10, 426-436.	10.4	42

#	Article	IF	CITATIONS
55	Electronic doping-enabled transition from n- to p-type conductivity over Au@CdS core–shell nanocrystals toward unassisted photoelectrochemical water splitting. Journal of Materials Chemistry A, 2019, 7, 23038-23045.	10.3	42
56	Synthesis of edge-site selectively deposited Au nanocrystals on TiO2 nanosheets: An efficient heterogeneous catalyst with enhanced visible-light photoactivity. Electrochimica Acta, 2018, 283, 1095-1104.	5.2	41
57	Evolution of Hollow CuInS <sub>2</sub> Nanododecahedrons via Kirkendall Effect Driven by Cation Exchange for Efficient Solar Water Splitting. ACS Applied Materials & Interfaces, 2019, 11, 27170-27177.	8.0	40
58	Au@HgxCd1-xTe core@shell nanorods by sequential aqueous cation exchange for near-infrared photodetectors. Nano Energy, 2019, 57, 57-65.	16.0	38
59	Bi/Zn Dual Singleâ€Atom Catalysts for Electroreduction of CO <sub>2</sub> to Syngas. ChemCatChem, 2022, 14, .	3.7	37
60	Oxygen Defects in Nanostructured <scp>Metalâ€Oxide</scp> Gas Sensors: Recent Advances and Challenges <sup>â€</sup> . Chinese Journal of Chemistry, 2020, 38, 1832-1846.	4.9	34
61	Controlled Synthesis and Flexible Self-Assembly of Monodisperse Au@Semiconductor Core/Shell Hetero-Nanocrystals into Diverse Superstructures. Chemistry of Materials, 2017, 29, 2355-2363.	6.7	33
62	Femtosecond laser mediated fabrication of micro/nanostructured TiO2- photoelectrodes: Hierarchical nanotubes array with oxygen vacancies and their photocatalysis properties. Applied Catalysis B: Environmental, 2020, 277, 119231.	20.2	33
63	Versatile synthesis of yolk/shell hybrid nanocrystals via ion-exchange reactions for novel metal/semiconductor and semiconductor/semiconductor conformations. Nano Research, 2017, 10, 2977-2987.	10.4	32
64	Engineering Acoustic Phonons and Electron–Phonon Coupling by the Nanoscale Interface. Nano Letters, 2015, 15, 6282-6288.	9.1	31
65	Dopant Diffusion Equilibrium Overcoming Impurity Loss of Doped QDs for Multimode Antiâ€Counterfeiting and Encryption. Advanced Functional Materials, 2021, 31, 2100286.	14.9	31
66	Synergetic Dualâ€Atom Catalysts: The Next Boom of Atomic Catalysts. ChemSusChem, 2022, 15, .	6.8	31
67	Core@shell sub-ten-nanometer noble metal nanoparticles with a controllable thin Pt shell and their catalytic activity towards oxygen reduction. Nano Research, 2015, 8, 271-280.	10.4	30
68	Mesoporous TiO2 microparticles formed by the oriented attachment of nanocrystals: A super-durable anode material for sodium-ion batteries. Nano Research, 2018, 11, 1563-1574.	10.4	30
69	Semiconductor Nanocrystal Engineering by Applying Thiol―and Solventâ€Coordinated Cation Exchange Kinetics. Angewandte Chemie - International Edition, 2019, 58, 4852-4857.	13.8	29
70	Design of a Singleâ€Atom Indium Î′+ –N 4 Interface for Efficient Electroreduction of CO 2 to Formate. Angewandte Chemie, 2020, 132, 22651-22655.	2.0	29
71	A flexible conductive film prepared by the oriented stacking of Ag and Au/Ag alloy nanoplates and its chemically roughened surface for explosive SERS detection and cell adhesion. RSC Advances, 2017, 7, 7073-7078.	3.6	28
72	An Aqueous Antiâ€Freezing and Heatâ€Tolerant Symmetric Microsupercapacitor with 2.3ÂV Output Voltage. Advanced Energy Materials, 2021, 11, 2101523.	19.5	28

#	Article	IF	CITATIONS
73	Theoretical Predictions, Experimental Modulation Strategies, and Applications of MXeneâ€&upported Atomically Dispersed Metal Sites. Small, 2022, 18, e2105883.	10.0	28
74	Redox shuttle enhances nonthermal femtosecond two-photon self-doping of rGO–TiO <sub>2â^'x</sub> photocatalysts under visible light. Journal of Materials Chemistry A, 2018, 6, 16430-16438.	10.3	27
75	Engineering the Local Atomic Environments of Indium Singleâ€Atom Catalysts for Efficient Electrochemical Production of Hydrogen Peroxide. Angewandte Chemie, 2022, 134, .	2.0	27
76	Simultaneous harnessing of hot electrons and hot holes achieved via n-metal-p Janus plasmonic heteronanocrystals. Nano Energy, 2022, 98, 107217.	16.0	26
77	From core-shell to yolk-shell: Keeping the intimately contacted interface for plasmonic metal@semiconductor nanorods toward enhanced near-infrared photoelectrochemical performance. Nano Research, 2020, 13, 1162-1170.	10.4	25
78	Cu x O self-assembled mesoporous microspheres with effective surface oxygen vacancy and their room temperature NO2 gas sensing performance. Science China Materials, 2018, 61, 1085-1094.	6.3	24
79	Orderly defective superstructure for enhanced pseudocapacitive storage in titanium niobium oxide. Nano Research, 2022, 15, 1570-1578.	10.4	24
80	From Cu2S nanocrystals to Cu doped CdS nanocrystals through cation exchange: controlled synthesis, optical properties and their p-type conductivity research. Science China Materials, 2015, 58, 693-703.	6.3	23
81	Oriented attachment of nanoparticles to form micrometer-sized nanosheets/nanobelts by topotactic reaction on rigid/flexible substrates with improved electronic properties. NPG Asia Materials, 2015, 7, e152-e152.	7.9	23
82	Atomically thin PdSeO <sub>3</sub> nanosheets: a promising 2D photocatalyst produced by quaternary ammonium intercalation and exfoliation. Chemical Communications, 2020, 56, 5504-5507.	4.1	23
83	RuO2 clusters derived from bulk SrRuO3: Robust catalyst for oxygen evolution reaction in acid. Nano Research, 2022, 15, 1959-1965.	10.4	23
84	Good Dispersion of Large-Stokes-Shift Heterovalent-Doped CdX Quantum Dots into Bulk PMMA Matrix and Their Optical Properties Characterization. Journal of Physical Chemistry C, 2017, 121, 6152-6159.	3.1	22
85	Synthesis of M-doped (M = Ag, Cu, In) Bi <sub>2</sub> Te <sub>3</sub> nanoplates <i>via</i> a solvothermal method and cation exchange reaction. Inorganic Chemistry Frontiers, 2019, 6, 1097-1102.	6.0	22
86	Compressive surface strained atomic-layer Cu2O on Cu@Ag nanoparticles. Nano Research, 2019, 12, 1187-1192.	10.4	21
87	Integrating Amorphous Molybdenum Sulfide Nanosheets with a Co <sub>9</sub> S <sub>8</sub> @Ni <sub>3</sub> S <sub>2</sub> Array as an Efficient Electrocatalyst for Overall Water Splitting. Langmuir, 2022, 38, 3469-3479.	3.5	21
88	Porous platinum–silver bimetallic alloys: surface composition and strain tunability toward enhanced electrocatalysis. Nanoscale, 2018, 10, 21703-21711.	5.6	20
89	Metal@I <sub>2</sub> –II–IV–VI <sub>4</sub> core–shell nanocrystals: controlled synthesis by aqueous cation exchange for efficient photoelectrochemical hydrogen generation. Journal of Materials Chemistry A, 2018, 6, 11898-11908.	10.3	20
90	From Indiumâ€Doped Ag <sub>2</sub> S to AgInS <sub>2</sub> Nanocrystals: Lowâ€Temperature In Situ Conversion of Colloidal Ag <sub>2</sub> S Nanoparticles and Their NIR Fluorescence. Chemistry - A European Journal, 2018, 24, 13676-13680.	3.3	20

#	Article	IF	CITATIONS
91	Phosphine ligand-mediated kinetics manipulation of aqueous cation exchange: a case study on the synthesis of Au@SnS <sub>x</sub> core–shell nanocrystals for photoelectrochemical water splitting. Chemical Communications, 2018, 54, 9993-9996.	4.1	19
92	Ultrafine PtRu Dilute Alloy Nanodendrites for Enhanced Electrocatalytic Methanol Oxidation. Chemistry - A European Journal, 2020, 26, 4025-4031.	3.3	19
93	Aqueous phase synthesis of Au@Ag <sub>3</sub> AuX <sub>2</sub> (X = Se, Te) core/shell nanocrystals and their broad NIR photothermal conversion application. CrystEngComm, 2016, 18, 5418-5422.	2.6	18
94	Unique Cation Exchange in Nanocrystal Matrix via Surface Vacancy Engineering Overcoming Chemical Kinetic Energy Barriers. CheM, 2020, 6, 3086-3099.	11.7	18
95	High-Performance Quantum Dots with Synergistic Doping and Oxide Shell Protection Synthesized by Cation Exchange Conversion of Ternary-Composition Nanoparticles. Journal of Physical Chemistry Letters, 2019, 10, 2606-2615.	4.6	17
96	Colloidal semiconductor nanocrystals for biological photodynamic therapy applications: Recent progress and perspectives. Progress in Natural Science: Materials International, 2020, 30, 443-455.	4.4	17
97	Atomic-dispersed platinum anchored on porous alumina sheets as an efficient catalyst for diboration of alkynes. Chemical Communications, 2020, 56, 3127-3130.	4.1	17
98	Recent Advances in Platinum-based Intermetallic Nanocrystals: Controlled Synthesis and Electrocatalytic Applications. Wuli Huaxue Xuebao/ Acta Physico - Chimica Sinica, 2020, .	4.9	17
99	Pure Aqueous Planar Microsupercapacitors with Ultrahigh Energy Density under Wide Temperature Ranges. Advanced Functional Materials, 2022, 32, .	14.9	17
100	Hollow anisotropic semiconductor nanoprisms with highly crystalline frameworks for high-efficiency photoelectrochemical water splitting. Journal of Materials Chemistry A, 2019, 7, 8061-8072.	10.3	16
101	Vacuum-tuned-atmosphere induced assembly of Au@Ag core/shell nanocubes into multi-dimensional superstructures and the ultrasensitive IAPP proteins SERS detection. Nano Research, 2019, 12, 1375-1379.	10.4	16
102	Ru-Co-Mn trimetallic alloy nanocatalyst driving bifunctional redox electrocatalysis. Science China Materials, 2022, 65, 131-138.	6.3	16
103	Hierarchical Self-Assembly of Cu <sub>7</sub> Te <sub>5</sub> Nanorods into Superstructures with Enhanced SERS Performance. ACS Applied Materials & Interfaces, 2016, 8, 35426-35434.	8.0	15
104	Intrinsic and Extrinsic Exciton Recombination Pathways in AgInS <sub>2</sub> Colloidal Nanocrystals. Energy Material Advances, 2021, 2021, .	11.0	15
105	Atomically dispersed Ru in Pt <sub>3</sub> Sn intermetallic alloy as an efficient methanol oxidation electrocatalyst. Chemical Communications, 2021, 57, 2164-2167.	4.1	14
106	Construction of Plasmonic Metal@Semiconductor Core–Shell Photocatalysts: From Epitaxial to Nonepitaxial Strategies. Small Structures, 2022, 3, .	12.0	13
107	Surface passivation enabled-structural engineering of I-III-VI <sub>2</sub> nanocrystal photocatalysts. Journal of Materials Chemistry A, 2020, 8, 9951-9962.	10.3	12
108	Layered Assembly of Silver Nanocubes/Polyelectrolyte/Gold Film as an Efficient Substrate for Surface-Enhanced Raman Scattering. ACS Applied Nano Materials, 2020, 3, 1934-1941.	5.0	12

#	Article	IF	CITATIONS
109	Shell Thickness Dependence of the Plasmon-Induced Hot-Electron Injection Process in Au@CdS Core–Shell Nanocrystals. Journal of Physical Chemistry C, 2021, 125, 19906-19913.	3.1	12
110	Ternary cooperative Au–CdS–rGO hetero-nanostructures: synthesis with multi-interface control and their photoelectrochemical sensor applications. RSC Advances, 2016, 6, 30785-30790.	3.6	11
111	Colloidâ€Interfaceâ€Assisted Laser Irradiation of Nanocrystals Superlattices to be Scalable Plasmonic Superstructures with Novel Activities. Small, 2018, 14, e1703501.	10.0	10
112	Micro-scale 2D quasi-nanosheets formed by 0D nanocrystals: from single to multicomponent building blocks. Science China Materials, 2020, 63, 1265-1271.	6.3	10
113	Fe-Functionalized α-Fe <sub>2</sub> O <sub>3</sub> /ZnO Nanocages for ppb-Level Acetone Gas Sensing. ACS Applied Nano Materials, 2022, 5, 5745-5755.	5.0	10
114	Telluride semiconductor nanocrystals: progress on their liquid-phase synthesis and applications. Rare Metals, 2022, 41, 2527-2551.	7.1	10
115	Cu nanocrystal enhancement of C <sub>3</sub> N <sub>4</sub> /Cu hetero-structures and new applications in photo-electronic catalysis: hydrazine oxidation and redox reactions of organic molecules. Inorganic Chemistry Frontiers, 2018, 5, 2420-2424.	6.0	9
116	Colloidal Cd <sub><i>x</i></sub> M <sub>1–<i>x</i></sub> Te Nanowires from the Visible to the Near Infrared Region: <i>N</i> , <i>N</i> -Dimethylformamide-Mediated Precise Cation Exchange. Journal of Physical Chemistry Letters, 2020, 11, 7-13.	4.6	9
117	Defect Engineering in 2D Photocatalytic Materials for CO <sub>2</sub> Reduction. ChemNanoMat, 2021, 7, 737-747.	2.8	9
118	Positively charged collective oscillations induce efficient Aβ1–42 fibril degradation in the presence of novel Au@Cu <sub>2â^'x</sub> S core/shell nanorods. Chemical Communications, 2021, 57, 6384-6387.	4.1	9
119	Semiconductor Nanocrystal Engineering by Applying Thiol―and Solventâ€Coordinated Cation Exchange Kinetics. Angewandte Chemie, 2019, 131, 4906-4911.	2.0	8
120	Stable quantum dots/polymer matrix and their versatile 3D printing frameworks. Journal of Materials Chemistry C, 2021, 9, 7194-7199.	5.5	8
121	A telluride shell on plasmonic Au nanoparticles: amorphous/crystalline phase and shape evolution engineering <i>via</i> aqueous cation exchange. Materials Chemistry Frontiers, 2021, 5, 4571-4578.	5.9	8
122	Colloidal Synthesis of Giant Shell PbSe-Based Core/Shell Quantum Dots in Polar Solvent: Cation Exchange versus Epitaxial Growth. Chemistry of Materials, 2020, 32, 6650-6656.	6.7	7
123	Telluride Nanocrystals with Adjustable Amorphous Shell Thickness and Core–Shell Structure Modulation by Aqueous Cation Exchange. Inorganic Chemistry, 2022, 61, 3989-3996.	4.0	7
124	A facile strategy to prepare monodisperse nanocrystals with initiative assembly into superlattice. Progress in Natural Science: Materials International, 2013, 23, 588-592.	4.4	6
125	Perovskite nanocrystals: across-dimensional attachment, film-scale assembly on a flexible substrate and their fluorescence properties. Nanotechnology, 2018, 29, 125606.	2.6	6
126	Cu-enhanced photoelectronic and ethanol sensing properties of Cu <sub>2</sub> O/Cu nanocrystals prepared by one-step controllable synthesis. Inorganic Chemistry Frontiers, 2018, 5, 425-431.	6.0	6

#	Article	IF	CITATIONS
127	Sharp-featured Au@Ag core/shell nanocuboid synthesis and the label-free ultrasensitive SERS detection of protein single-point mutations. Materials Chemistry Frontiers, 2018, 2, 1720-1724.	5.9	6
128	Optical and electrical properties of carbon nitride films deposited by cathode electrodeposition. Journal of Materials Science, 2003, 38, 2559-2562.	3.7	5
129	P-type Cu <sub>7</sub> Te <sub>5</sub> single-crystalline nanocuboids: size-controlled synthesis and large-scale self-assembly. CrystEngComm, 2014, 16, 9441-9445.	2.6	5
130	Aqueous oxidation reaction enabled layer-by-layer corrosion of semiconductor nanoplates into single-crystalline 2D nanocrystals with single layer accuracy and ionic surface capping. Chemical Communications, 2016, 52, 3426-3429.	4.1	5
131	Nanoclusterâ€Mediated Synthesis of Diverse ZnTe Nanostructures: from Nanocrystals to 1D Nanobelts. Chemistry - A European Journal, 2018, 24, 2999-3004.	3.3	5
132	Nearâ€Infrared Luminescent Ternary Ag <sub>3</sub> SbS <sub>3</sub> Quantum Dots by in situ Conversion of Ag Nanocrystals with Sb(C <sub>9</sub> H <sub>19</sub> COOS) <sub>3</sub> . Chemistry - A European Journal, 2018, 24, 18643-18647.	3.3	5
133	High Pressure Induced in Situ Solid-State Phase Transformation of Nonepitaxial Grown Metal@Semiconductor Nanocrystals. Journal of Physical Chemistry Letters, 2018, 9, 6544-6549.	4.6	5
134	Cation Exchange Enabled Cu Dopants Location Tailoring and Photoelectric Properties Regulation in CdS Nanosheets. Journal of Physical Chemistry Letters, 2021, 12, 3976-3982.	4.6	5
135	Doping transition metal in PdSeO3 atomic layers by aqueous cation exchange: A new doping protocol for a new 2D photocatalyst. Chinese Chemical Letters, 2022, 33, 3739-3744.	9.0	5
136	Synergistically Modulating Geometry and Electronic Structures of a Chalcogenide Photocatalyst via an Ion-Exchange Strategy. Journal of Physical Chemistry Letters, 2022, 13, 969-976.	4.6	5
137	Microreactor platform for continuous synthesis of electronic doped quantum dots. Nano Research, 2022, 15, 9647-9653.	10.4	5
138	Noble Metal-Based Nanocomposites for Fuel Cells. , 2018, , .		4
139	Assembly-promoted photocatalysis: Three-dimensional assembly of CdS x Se 1â^'x (xÂ=Â0–1) quantum dots into nanospheres with enhanced photocatalytic performance. Journal of Materiomics, 2017, 3, 63-70.	5.7	3
140	Two-dimensional CdX (X = Se, Te) nanosheets: controlled synthesis and their photoluminescence properties. Journal of Materials Chemistry C, 2019, 7, 13849-13858.	5.5	3
141	Computational Studies of Coinage Metal Anion Mâ^' + CH3X (X = F, Cl, Br, I) Reactions in Gas Phase. Molecules, 2022, 27, 307.	3.8	3
142	Siteâ€Specific Growth of Au on CdS <i><sub>x</sub></i> Se <sub>1â^'</sub> <i><sub>x</sub></i> Yields Anisotropic Heteronanocrystals with Enhanced Photocatalysis Performance. Particle and Particle Systems Characterization, 2016, 33, 512-518.	2.3	2
143	Editorial for rare metals, special issue on nanomaterials and rechargeable battery applications. Rare Metals, 2017, 36, 305-306.	7.1	2
144	Precisely Controllable Synthesized Nanoparticles for Surface Enhanced Raman Spectroscopy. , 0, , .		2

#	Article	IF	CITATIONS
145	Luminescent Cu doped CdTe nanocrystals via cation exchange of Cu7Te5 nanocubes: From undoped to doped emission. Progress in Natural Science: Materials International, 2021, 31, 398-403.	4.4	2
146	Wet-Phase Synthesis of Typical Magnetic Nanoparticles with Controlled Morphologies. , 2017, , 291-326.		1
147	Phase transformation of PiMoCo and their electrocatalytic activity for oxygen evolution reaction. CrystEngComm, 2020, 22, 6003-6009.	2.6	1
148	Surface-Enhanced Raman Scattering Quantitative Analysis of Ethanol Drop-Coating Silver Nanocubes on Gold Film. Journal of Nanoscience and Nanotechnology, 2021, 21, 4715-4725.	0.9	1
149	Atomically Surficial Modulation in Two-Dimensional Semiconductor Nanocrystals for Selective Photocatalytic Reactions. Frontiers in Chemistry, 2022, 10, 890287.	3.6	1
150	Cation coordination reactions on nanocrystals: surface/interface, doping control and advanced photocatalysis applications (Conference Presentation). , 2016, , .		0
151	Yolk / Shell Nanocrystals: A Novel Approach To Catalysis and Drug Release. , 2017, , .		0
152	Synthesis of multicomponent colloidal nanoparticles. , 2022, , .		0